



Cite this: *Chem. Commun.*, 2026, 62, 231

Received 6th October 2025,
Accepted 20th November 2025

DOI: 10.1039/d5cc05684e

rsc.li/chemcomm

One-pot synthesis of novel triazine/piperazine-based macrocycles and investigation of their porous properties

Ho-Yin Lai,^a Yao-Chih Lu,^a Hsiang-Jen Cheng,^b Hsiu-Fu Hsu^{ID *b} and Long-Li Lai^{ID *a}

Four macrocycles with the penta-triazine and penta-piperazine scaffold were efficiently synthesized via self-cyclization in 15–23% yields; the synthesized macrocycles were assumed to have crown-shaped conformations by NMR spectroscopy and computational simulations and contain void spaces in the bulky state by CO₂ isotherms.

Macrocycles have attracted considerable attention and have been extensively investigated in recent decades owing to their unique molecular conformations and intriguing biological properties, but their synthesis often remains challenging.¹ These challenges have been addressed and overcome in several well-established systems, such as cyclodextrins, calixarenes, and porphyrins.² Consequently, macrocycles can be systematically studied with respect to their related physico-chemical properties.³ Trichlorotriazine is not only inexpensive but also quite reactive toward nucleophiles, making it an excellent building block for the synthesis of triazine-based macrocycles.⁴ Moreover, triazine derivatives have been widely explored in the development of herbicides⁵ and medicinal chemistry.⁶ Due to the strong π - π stacking and hydrogen-bonding interactions between triazine units,⁷ triazine-containing moieties have also been employed in the construction of dendritic and polymeric molecules, which often display liquid-crystalline behaviour or gas-adsorption properties.⁸ Although triazine-based macrocycles have been synthesized⁹ and employed as potential molecular receptors in solution,^{9a–c} reports on their gas-adsorption functionality remain scarce.^{9f,g}

On the other hand, metal-organic frameworks (MOFs),¹⁰ covalent-organic frameworks (COFs),¹¹ and porous organic polymers (POPs)¹² have been extensively investigated as representative porous materials. However, their recrystallization or purification after use is still of concern due to their poor

solubility in common solvents.¹³ Although hydrogen-bonded organic frameworks (HOFs) do not suffer from this solubility issue, they are generally unstable, and their cavities often collapse or shrink significantly upon solvent evaporation.^{9f,14}

Thus, the development of macrocycles that exhibit good solubility in organic solvents and also function as porous materials is highly desirable. Such macrocycles not only enable efficient purification after synthesis but also facilitate reprocessing after usage. Moreover, the intrinsic cavities within these macrocycles can serve as hosts for guest molecules in the solid and solution states.¹⁵ In this work, we first synthesized compounds **2a–2d**, which underwent self-cyclization to afford the corresponding macrocycles **3a–3d** with the penta-triazine and penta-piperazine [5T+5P] scaffold in 15–23% yields. Macrocycle **3b**, as a representative member of this series, was further investigated in the solid state by CO₂ adsorption isotherms. We now report these results.

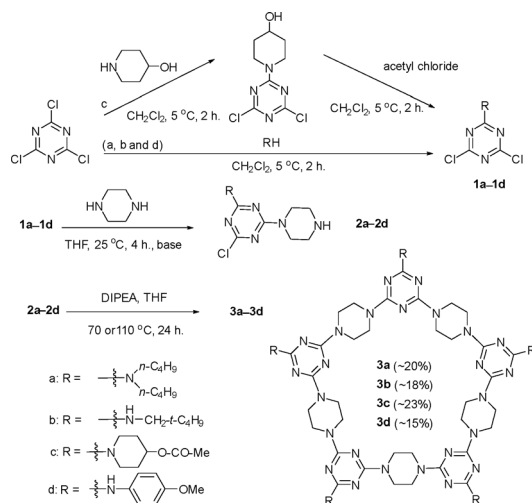
Compounds **2a–2d**, serving as precursors to the target macrocycles, were efficiently synthesized following the reported procedure (Scheme 1).^{4b,c,9h} Macrocycles **3a–3c** were subsequently obtained from **2a–2c**, respectively, by self-cyclization at 70 °C. In contrast, a higher temperature of 110 °C was required to completely convert **2d** into **3d**. It is noteworthy that compounds **2a–2d**, which contain both electron-donating and electron-withdrawing substituents, were found to undergo slight decomposition either in solution or in the solid state and were therefore employed directly in the subsequent cyclization immediately after preparation.

As mentioned previously, macrocycles featuring a tri-triazine/tri-piperazine [3T+3P] scaffold have been prepared via combinatorial synthesis as potential molecular receptors.^{9h} This observation prompted us to target the synthesis of triazine- and piperazine-based macrocycles with larger [5T+5P] scaffolds, which possess significantly larger cavities and are expected to exhibit more diverse host–guest recognition capabilities. However, the stepwise synthetic route employing protection–deprotection strategies reported in the literature

^a Department of Applied Chemistry, National Chi Nan University, Puli, Nantou, 545, Taiwan. E-mail: lilai@ncnu.edu.tw

^b Department of Chemistry, Tamkang University, Tamsui, 251, Taiwan





Scheme 1 Synthesis of macrocycles **3a–3d** from precursors **2a–2d** via self-cyclization.

for the preparation of [3T+3P] macrocycles^{9h} is not well suited for the synthesis of macrocycles **3a–3d**. The approach to construct the larger macrocycles *via* self-cyclization from precursors **2a–2d** should greatly simplify the synthesis as shown in Scheme 1.

The multistep procedures containing protection and deprotection are rather laborious and may give the targeted macrocycles in very low yields. Additionally, they may be costly because lots of solvents and silica may be used in purification. In addition to the stepwise [3T+3P] systems,^{9h} another macrocyclic framework containing triazine and piperazine units with a [6T+6P] scaffold has been reported as an intermediate in the one-pot synthesis of covalent organic polymers (COPs).¹⁶ However, this hexagonal macrocyclic scaffold, either presented as an intermediate or within COPs, was not spectroscopically confirmed but was merely proposed as the thermodynamically stable structure. Instead of the [6T+6P] scaffold,¹⁶ the [5T+5P] scaffold was obtained for **3a–3d** in our synthesis, as directly evidenced by high-resolution mass spectrometry (HRMS), and further indirectly confirmed by nuclear magnetic resonance (NMR) analyses. HRMS analysis of **3a** revealed a molecular ion peak at *m/z* 1452.1137 with an isotope distribution matching the theoretically calculated pattern for the cyclic [5T+5P] framework (Fig. S1). The HRMS spectra of **3b–3d** are also provided in Fig. S1.

The ¹H NMR spectrum of **3a** (Fig. 1), which displays a single resonance for each type of proton, indicates a highly symmetrical molecular structure. Similarly, the ¹³C NMR spectrum (Fig. S2) exhibits signals consistent with a symmetric framework, in agreement with the ¹H NMR observations. These spectroscopic results collectively support the cyclic structure of **3a–3d**, which should have a [5T+5P] scaffold further on the analysis of HRMS.

The conformation of the macrocycle was further investigated by ¹H NMR spectroscopy. The axial-equatorial interconversion of the CH₂ units and chair-boat interconversion of the

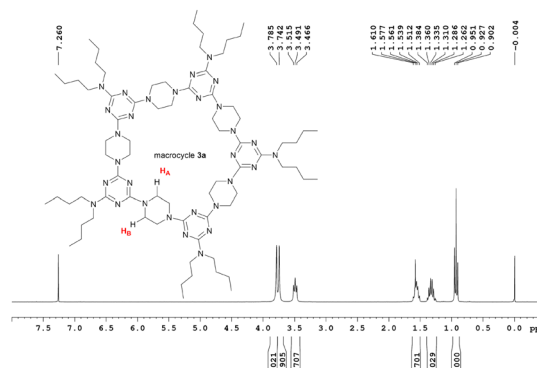


Fig. 1 The ¹H-NMR spectra (300 MHz, CDCl₃) of macrocycle **3a**.

piperazine in planar macrocycles have been reported to be rapid even at temperatures as low as 203 K.¹⁷ At room temperature, the two distinct resonances observed at 3.79 and 3.75 ppm for the piperazine CH₂ protons (H_A and H_B) do not arise from the axial-equatorial and chair-boat interconversion, but indicate that these protons reside in non-equivalent chemical environments, implying the nonplanar conformation of macrocycle **3a**. A high energy barrier for inversion of the crown conformation¹⁸ is expected to result in two inequivalent piperazine CH₂ environments, with H_A located inside the crown and H_B positioned outside (Fig. 1).

Variable-temperature ¹H NMR spectra of **3a** recorded between 20 and -60 °C in the 0.6–4.4 ppm region (Fig. S3) also showed that the axial-equatorial and chair-boat interconversion of the piperazine CH₂ units in a non-planar macrocycle is also rapid, as that observed in a planar macrocycle.¹⁷ This further confirms that the resonances at 3.79 and 3.75 ppm actually arise from non-equivalent chemical environments of Hs. In the ¹³C NMR spectrum collected at room temperature (Fig. S2), two distinct signals were also observed for the piperazine CH₂ carbons at 43.18 and 43.34 ppm (C_A and C_B), further supporting the presence of two chemically non-equivalent CH₂ environments. These findings are consistent with the optimized crown-shaped conformation and corroborate the conclusions drawn from ¹H NMR analysis.

To gain structural insights, macrocycle **3a** was subjected to theoretical calculations for geometry optimization and heat of formation. Calculations were performed using the CaChe program with the MM2 force field¹⁹ and density functional theory (DFT) in the gas phase. In addition to **3a** with a [5T+5P] scaffold, the analogous macrocycle with a [6T+6P] scaffold was also simulated (Fig. 2). Both MM2 and DFT calculations converged to a crown-shaped conformation for the [5T+5P] macrocycle and a nearly planar conformation for the [6T+6P] macrocycle (Fig. S4 and S5).

For macrocycles bearing identical peripheral groups, R = N(C₄H₉)₂, the calculated formation energies of the [5T+5P] and [6T+6P] scaffolds were 0.108 and 0.107 kcal·mmol⁻¹·atom⁻¹, respectively. The corresponding total energies were -12 112 and -12 218 kcal·mmol⁻¹·atom⁻¹ using the B3LYP functional with the 6-311+G** basis set (Table S1).²⁰ Both the MM2 and



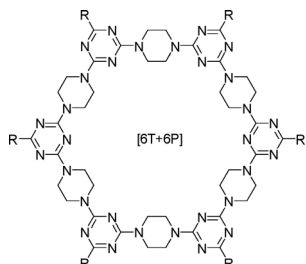


Fig. 2 The triazine- and piperazine-based macrocycles with the [6T+6P] scaffold.

DFT results are in good agreement, indicating that the [6T+6P] macrocycle is only slightly more thermodynamically stable than the [5T+5P] macrocycle. These results suggest that the preferential formation of [5T+5P] macrocycles is governed by kinetic rather than thermodynamic control.

Furthermore, conformers of **3a** with varying ratios of chair/boat forms in the piperazine units were also calculated, with results summarized in Tables S2, S3 and Fig. S6. The calculations revealed that each conversion from a chair to a boat conformation required approximately $2.7 \text{ kcal}\cdot\text{mol}^{-1}$. Among all eight possible chair/boat conformers, the fully chair conformation **3a** with crown shape was found to be the most thermodynamically stable.

The ^1H and ^{13}C NMR spectra of **3b**–**3d** (Fig. S7 and S8) further support the nonplanar conformation of these macrocycles. For **3c** and **3d**, two distinct resonances were observed at approximately 3.79 and 3.75 ppm, consistent with the presence of two chemically non-equivalent piperazine CH_2 environments. In the case of **3b**, a broadened signal for the piperazine CH_2 protons was detected near 3.79 ppm. This broadening can be attributed to a more dynamic conformation, likely arising from the reduced steric hindrance of its peripheral substituents.

The thermal stability of macrocycle **3a** was evaluated by thermogravimetric analysis (TGA). Compound **3a** exhibited thermal stability up to 280°C (Fig. S9). The slight weight loss observed is attributed to solvent evaporation during heating, further supporting the presence of a porous framework in the bulky state. Similar TGA profiles were obtained for compounds **3b**–**3d** (Fig. S9).

The porous properties of **3b**, as a representative compound of this series, were further investigated by CO_2 adsorption isotherms measured at 195, 273, and 298 K (Fig. 3a). The Brunauer–Emmett–Teller (BET) surface area²¹ of **3b** was determined to be $154.2 \text{ m}^2\cdot\text{g}^{-1}$ (Langmuir surface area: $193.0 \text{ m}^2\cdot\text{g}^{-1}$) based on the CO_2 isotherm at 195 K, which is comparable with that of a porous triazine-based macrocycle.⁹ The pore size distribution of **3b** in the bulk state was calculated from the CO_2 isotherm of 273 K using the DFT model (density functional theory model) according to the literature,²² which falls within the range of 4.5–8.5 Å (Fig. 3b). Based on the conformation of **3b** without considering the peripheral substituents, the rim-to-rim distances in larger and smaller openings of crown-shape molecules are between 5.6 and 11.7 Å

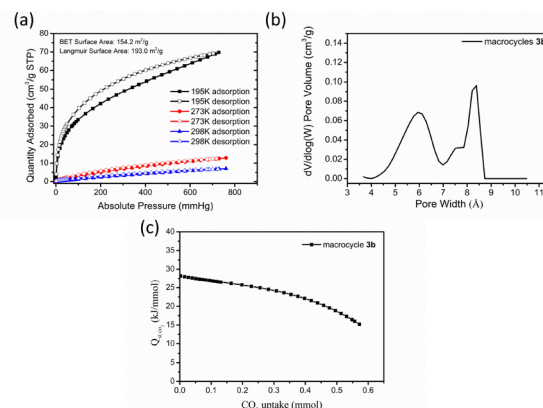


Fig. 3 (a) The CO_2 isotherms of macrocycle **3b** at 195, 273 and 298 K. (b) The pore size distribution of **3b** based on the CO_2 isotherm at 273 K. (c) Q_{st} for **3b** derived from the adsorption isotherms at 273 and 298 K.

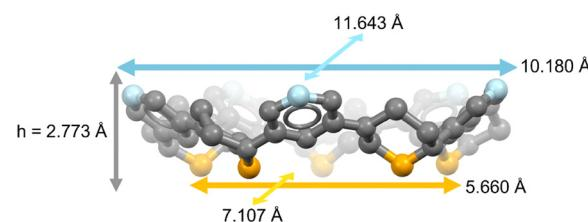


Fig. 4 The height and rim-to-rim distances in the upper and lower openings of the crown-shape molecule.

(Fig. 4), which indicates the rationality of pore size distribution from the CO_2 isotherm of 273 K.

From the CO_2 isotherms collected at 273 and 298 K, the isosteric heat of adsorption (Q_{st}) of **3b** was calculated to be approximately $28.2 \text{ kJ}\cdot\text{mol}^{-1}$ at zero coverage and was observed to decrease progressively with increasing CO_2 loading, as determined by the virial method (Fig. 3c).²³ This trend can be rationalized by the preferential occupation of the strongest adsorption sites at low coverage, likely located near the triaminotriazine cores of **3b**, where strong polar–polar interactions occur between CO_2 molecules and triaminotriazine moieties.²⁴ Consequently, Q_{st} is initially high but decreases significantly as the nitrogen-containing sites become saturated with CO_2 .²⁵

In summary, four triazine- and piperazine-based macrocycles with [5T+5P] scaffolds were successfully synthesized via a self-cyclization strategy, thereby eliminating the need for repetitive protection–deprotection steps. HRMS analysis confirmed the molecular compositions, while NMR spectroscopy and computational simulations indicated that macrocycles **3a**–**3d** adopt crown-shaped conformations. The porosity of **3b** was further demonstrated through surface area measurements and pore-size distribution analysis by CO_2 adsorption. Collectively, these results establish a straightforward and efficient synthetic approach to access triazine–piperazine macrocycles with large internal cavities, which hold promise for future host–guest and adsorption-related applications.



Conflicts of interest

There are no conflicts to declare.

Data availability

The data supporting this article have been included as part of the supplementary information (SI). Supplementary information: synthetic details and characterization data. See DOI: <https://doi.org/10.1039/d5cc05684e>.

Notes and references

- (a) E. M. Driggers, S. P. Hale, J. Lee and N. K. Terrett, *Nat. Rev. Drug Discovery*, 2008, **7**, 608–624; (b) M. Stępień, N. Sprutta and L. Łatoss-Grażyński, *Angew. Chem., Int. Ed.*, 2011, **50**, 4288–4340; (c) K. Jie, Y. Zhou, E. Li and F. Huang, *Acc. Chem. Res.*, 2018, **51**, 2064–2072; (d) X.-X. Jia, S.-P. Tao, Y.-M. Huang, T.-B. Wei, B. Shi, Q. Lin, H. Yao and J.-F. Chen, *Org. Lett.*, 2025, **27**, 11231–11236.
- (a) W. Tang and S.-C. Ng, *Nat. Protoc.*, 2008, **3**, 691–697; (b) A. R. Khan, P. Forgo, K. J. Stine and V. T. D’Souza, *Chem. Rev.*, 1998, **98**, 1977–1996; (c) H. J. Kim, M. H. Lee, L. Mutihac, J. Vicens and J. S. Kim, *Chem. Soc. Rev.*, 2012, **41**, 1173–1190; (d) G. S. Ananchenko, I. L. Moudrakovski, A. W. Coleman and J. A. Ripmeester, *Angew. Chem., Int. Ed.*, 2008, **47**, 5616–5618; (e) I. Kim, A. Dhamija, I.-C. Hwang, H. Lee, Y. H. Ko and K. Kim, *Chem. – Asian J.*, 2021, **16**, 3209–3212; (f) W. Yang, F. Yang, T.-L. Hu, S. C. King, H. Wang, H. Wu, W. Zhou, J.-R. Li, H. D. Arman and B. Chen, *Cryst. Growth Des.*, 2016, **16**, 5831–5835.
- M. Iyoda, J. Yamakawa and M. J. Rahman, *Angew. Chem., Int. Ed.*, 2011, **50**, 10522–10553.
- (a) G. Giacomelli, A. Porcheddu and L. D. Luca, *Curr. Org. Chem.*, 2004, **8**, 1497–1519; (b) W. J. Schnabel, R. Rätz and E. Kober, *J. Org. Chem.*, 1962, **27**, 2514–2519; (c) J. T. Thurston, J. R. Dudley, D. W. Kaiser, I. Hechenbleikner, F. C. Schaefer and D. Holm-Hansen, *J. Am. Chem. Soc.*, 1951, **73**, 2981–2983.
- G. Muller, H. LeBaron, J. McFarland and O. Burnside, History of the discovery and development of triazine herbicides, 2008.
- M. Vidal-Mosquera, A. Fernández-Carvajal, A. Moure, P. Valente, R. Planells-Cases, J. M. González-Ros, J. Bujons, A. Ferrer-Montiel and A. Messeguer, *J. Mater. Chem.*, 2011, **54**, 7441–7452.
- P. Gamez and J. Reedijk, *Eur. J. Inorg. Chem.*, 2006, 29–42.
- (a) L.-L. Lai, C.-H. Lee, L.-Y. Wang, K.-L. Cheng and H.-F. Hsu, *J. Org. Chem.*, 2008, **73**, 485–490; (b) L.-L. Lai, S.-J. Hsu, H.-C. Hsu, S.-W. Wang, K.-L. Cheng, C.-J. Chen, T.-H. Wang and H.-F. Hsu, *Chem. – Eur. J.*, 2012, **18**, 6542–6547; (c) L.-L. Lai, J.-W. Hsieh, K.-L. Cheng, S.-H. Liu, J.-J. Lee and H.-F. Hsu, *Chem. – Eur. J.*, 2014, **20**, 5160–5166; (d) M.-J. Tsai, J.-W. Hsieh, L.-L. Lai, K.-L. Cheng, S.-H. Liu, J.-J. Lee and H.-F. Hsu, *J. Org. Chem.*, 2016, **81**, 5007–5013; (e) C.-H. Lee, C.-C. Huang, C.-Y. Li, L.-L. Lai, J.-J. Lee and H.-F. Hsu, *J. Mater. Chem. C*, 2019, **7**, 14232–14238; (f) Y.-C. Lu, H.-F. Hsu and L.-L. Lai, *Nanomaterials*, 2021, **11**, 2112; (g) Y.-C. Lu, R. Anedda,
- (a) D.-X. Wang, Q.-Y. Zheng, Q.-Q. Wang and M.-X. Wang, *Angew. Chem., Int. Ed.*, 2008, **47**, 7485–7488; (b) J. M. Caio, T. Esteves, S. Carvalho, C. Moiteiro and V. Félix, *Org. Biomol. Chem.*, 2014, **12**, 589–599; (c) S. Bozkurt and M. B. Türkmen, *Tetrahedron: Asymmetry*, 2016, **27**, 443–447; (d) M.-X. Wang and H.-B. Yang, *J. Am. Chem. Soc.*, 2004, **126**, 15412–15422; (e) H. Zhang, Y.-F. Ao, D.-X. Wang and Q.-Q. Wang, *J. Org. Chem.*, 2022, **87**, 3491–3497; (f) Y.-C. Lu, C.-H. Lee, H.-H. Kuo, H.-C. Chiang, C.-T. Yao, H.-L. Sung, G.-H. Lee and L.-L. Lai, *Cryst. Growth Des.*, 2020, **20**, 6421–6429; (g) Z.-T. Gu, H.-C. Chen, J.-P. Yang, H.-F. Hsu, T.-S. Kuo and L.-L. Lai, *Chem. Commun.*, 2024, **60**, 14830–14833; (h) D. W. P. M. Löwik and C. R. Lowe, *Tetrahedron Lett.*, 2000, **41**, 1837–1840.
- (a) S. Tashiro and M. Shionoya, *Acc. Chem. Res.*, 2020, **53**, 632–643; (b) G. Zhang, B. Hua, A. Dey, M. Ghosh, B. A. Moosa and N. M. Khashab, *Acc. Chem. Res.*, 2021, **54**, 155–168.
- (a) A. Yepremyan, A. Mahmood, P. Asgari, B. G. Janesko and E. E. Simanek, *ChemBioChem*, 2019, **20**, 241–246; (b) A. Schoedel, M. Li, D. Li, M. O’Keeffe and O. M. Yaghi, *Chem. Rev.*, 2016, **116**, 12466–12535.
- G. Zhang, M. Tsujimoto, D. Packwood, N. T. Duong, Y. Nishiyama, K. Kadota, S. Kitagawa and S. Horike, *J. Am. Chem. Soc.*, 2018, **140**, 2602–2609.
- T. Dutta, T. Kim, K. Vellingiri, D. C. W. Tsang, J. R. Shon, K.-H. Kim and S. Kumar, *Chem. Eng. J.*, 2019, **364**, 514–529.
- (a) C.-H. Lee, D. V. Soldatov, C.-H. Tzeng, L.-L. Lai and K.-L. Lu, *Sci. Rep.*, 2017, **7**, 3649; (b) Y.-C. Lu, C.-Y. Chien, H.-F. Hsu and L.-L. Lai, *Molecules*, 2021, **26**, 4862.
- I. Hisaki, *J. Inclusion Phenom. Macroyclic Chem.*, 2020, **96**, 215–231.
- H. A. Patel, F. Karadas, A. Canlier, J. Park, E. Deniz, Y. Jung, M. Atilhan and C. T. Yavuz, *J. Mater. Chem.*, 2012, **22**, 8431–8437.
- C.-C. Lee, M. Usman, M.-Y. Kuo, P. Thanasekaran, C.-C. Liu, J.-Y. Wu, G. R. Chiou, J.-W. Chen, C.-H. Lee, L.-W. Lee, Y.-H. Pan, L.-L. Lai, C.-H. Hung and K.-L. Lu, *Chem. – Asian J.*, 2025, e00463.
- G.-Y. Wu, C.-L. Huang, H.-W. Kang, W.-T. Ou, Y.-S. Ho, M.-J. Cheng and Y.-T. Wu, *Angew. Chem., Int. Ed.*, 2024, **63**, e202408321.
- N. L. Allinger, *J. Am. Chem. Soc.*, 1977, **99**, 8127–8134.
- (a) P. Hohenberg and W. Kohn, *Phys. Rev.*, 1964, **136**, B864; (b) W. Kohn and L. J. Sham, *Phys. Rev.*, 1965, **140**, A1133–A1138.
- J.-B. Lin, J.-P. Zhang and X.-M. Chen, *J. Am. Chem. Soc.*, 2010, **132**, 6654–6656.
- J. Landers, G. Y. Gor and A. V. Neimark, *Colloids Surf. A*, 2013, **437**, 3–32.
- (a) H. Pan, J. A. Ritter and P. B. Balbuena, *Langmuir*, 1998, **14**, 6323–6327; (b) A. Zukal, J. Pawlesa and J. Čejka, *Adsorption*, 2009, **15**, 264–270.
- L.-L. Lai, H.-C. Hsu, S.-J. Hsu and K.-L. Cheng, *Synthesis*, 2010, 3576–3582.
- M. G. Rabbani, T. Islamoglu and H. M. El-Kaderi, *J. Mater. Chem. A*, 2017, **5**, 258–265.

